Geometrically controlled liquefied capsules for modular tissue engineering strategies

Sara Nadine, Sónia G. Patrício, Cristina C. Barrias, Insung S. Choi, Michiya Matsusaki, Clara R. Correia, João F. Mano**

S. Nadine, Dr. S. G. Patrício, Dr. C. R. Correia, Prof. J. F. Mano
CICECO – Aveiro Institute of Materials, Department of Chemistry, University of Aveiro, Campus Universitário de Santiago, 3810-193 Aveiro, Portugal
E-mail: claracorreia@ua.pt and jmano@ua.pt

Dr. C. C. Barrias
i3S, Instituto De Investigação e Inovação Em Saúde, Universidade Do Porto, Rua Alfredo Allen, 208, 4200-135 Porto, Portugal

Dr. C. C. Barrias
INEB, Instituto De Engenharia Biomédica, Universidade Do Porto, Rua Alfredo Allen, 208, 4200-135 Porto, Portugal

Dr. C. C. Barrias
ICBAS, Instituto De Ciências Biomédicas Abel Salazar, Universidade Do Porto, Rua De Jorge Viterbo Ferreira, 228, 4050-313 Porto, Portugal

Prof. I. S. Choi
Center for Cell-Encapsulation Research, Department of Chemistry, KAIST, Daejeon, 34141 South Korea

Prof. M. Matsusaki
Division of Applied Chemistry Graduate School of Engineering Osaka University 2-1 Yamadaoka, Suita, Osaka 565-0871, Japan

Keywords: Liquefied Capsules, Modular Tissue Engineering, Microparticles, Stem Cells, Geometrically-controlled Microgels

A plethora of bioinspired cell-laden hydrogels are being explored as building blocks that once assembled are able to create complex and highly hierarchical structures recapitulating the heterogeneity of living tissues. Yet, the resulting 3D bioengineered systems still present key limitations, mainly related with limited diffusion of essential molecules for cell survival, which dictates the failure of most strategies upon implantation. To maximize the hierarchical complexity of bioengineered systems, while simultaneously fully addressing the exchange efficiency of biomolecules, we propose the high-throughput fabrication of liquefied capsules

using superhydrophobic-superhydrophilic microarrays as platforms to produce the initial structures with high fidelity of geometry and size. The liquefied capsules are composed by (i) a permselective multilayered membrane; (ii) surface functionalized poly(ε-caprolactone) microparticles loaded into the liquefied core acting as cell adhesion sites; and (iii) cells. We demonstrate that besides the typical spherical liquefied capsules, it is also possible to obtain multi-shaped blocks with high geometrical precision and efficiency. Importantly, the internal gelation approach used to produce such blocks did not jeopardize cell viability, evidencing the mild conditions of the proposed cell encapsulation technique. We intend to use the proposed system as hybrid devices implantable by minimally invasive procedures for multiple tissue engineering applications.

Tissue Engineering (TE) approaches aim to restore or replace the function of tissues or organs with compromised self-repairing capability. The strategy combines autologous cells with instructive biomaterials to recreate living and functional engineered tissues. Living tissues are characterized by repetitive functional units, which include combinations of heterogeneous cell populations and extracellular matrix (ECM), structured across multiple length scales. In an attempt to mimic such hierarchical, adaptive and complex functionality and spatial organization, the assemble of 3D functional units with defined microarchitectural features was envisaged, in a concept termed modular TE.[1,2] In modular TE approaches, cell-laden hydrogels are being considerably explored as building blocks to create modular tissues with specific geometries and mechanical properties.[3,4] Hydrogels are attractive 3D cell supportive platforms due to their highly hydrated nature, resembling the tissue-like compliance of the native ECM.[5] Cell-laden modular units enable the spatial and temporal manipulation of the biomaterials microenvironment, while avoid the invasive procedures inherent to scaffolds implantation into a defect site. Once created, the modular units can be assembled into larger multifunctional tissues, structured in a scale-range manner. Each modular unit can carry

distinct cargo, including multiphenotypic cells and biomolecules of interest. The assembly of 3D modular units was already proposed for the fabrication of different tissues, such as cartilage[6], hepatic[7], and heart tissues[8]. While spherical systems are the most widely used, the generation of multi-shaped complex 3D structures are being increasingly explored to mimic the complexity of native tissues.[9] For example, cylinder-shaped microgels can be projected to resemble structures of the human body, such as muscle fibers[10] or blood vessels[11].

Despite the favorable properties of hydrogels as 3D cell encapsulation systems, macroscopic hydrogels, as those arised from the assemble of modular units, still present key issues, namely limited cell-cell contact and signalling, as well as poor mass transportation of essential molecules.[12] Generally, cell death occurs at the inner regions of hydrogels, dictating their poor *in vivo* performance.[13] Furthermore, most hydrogels require modification of the polymeric matrix to enhance their cell adhesive properties, as most cells are anchorage dependent, thus undergoing anoikis when deprived from a physical support.[14] To overcome the drawbacks related with cell-laden hydrogels, we propose the development of a disruptive cell encapsulation system allowing production at high rate and with defined sizes and shapes using the effect of discontinuous dewetting on a superhydrophobic-superhydrophilic microarray. The concept proposed relies on producing alginate-based microgels with controlled geometry, using an internal crosslinking procedure, coating them with a permselective polymeric layer and liquefying the core – see **Scheme 1**. The final liquefied capsules are generically composed by (i) a multilayered membrane, obtained through the layer-by-layer technique; (ii) surface functionalized poly(ε-caprolactone) microparticles (μPCL) loaded into the liquefied core; and (iii) cells. While the multilayered membrane wraps all the cargo content and ensures the high diffusion of essential molecules for cell survival, the microparticles act as cell adhesion sites, allowing cells to adhere and proliferate, and eventually differentiate when stem/progenitor cells are used.[15,16] The advantages of using

microparticles as cell carriers are well-documented. In particular, liquefied cell encapsulation systems containing microparticles presented an enhanced metabolic activity (MTS colorimetric assay) and cell proliferation (DNA quantification) compared to liquefied capsules without microparticles. Additionally, the encapsulation of microparticles avoids the limitations inherent to cell spheroids, such as the existence of hypoxia regions, which consequently often leads to necrotic cores.[12] Importantly, the unique liquefied environment of the system allows to create dynamic flows within the core microenvironment, maximizing the interaction of cells with microparticles, and the dispersion of important biomolecules, including nutrients, oxygen, growth factors and cytokines, through the entire 3D construct. Previously, we hypothesized that a mechanical stimulation added to the culture of liquefied capsules could increase the interactions between cells and microparticles while improving mass transfer inside the compartmentalized capsules. Results demonstrated that the interactions of the cellular components were enhanced by the hydrodynamic shear provided by the uniform and continuous rotation of the culture medium. In fact, the fluid flow drove cells to adhere to the surface of the microparticles, to proliferate, and to deposit a complex collagen-rich extracellular matrix in such a way that microparticles were assembled in 3D micro-constructs.[17]

Herein, we intend to take advantage of the key features that liquefied and multilayered capsules bring to cell encapsulation systems aiming tissue repair, by proposing millimeter-sized geometrically shaped modular systems. For that, a versatile technique was used for the high-throughput fabrication of freestanding microgels encapsulating cells and µPCL. Techniques using superhydrophobic substrates have been used in biomedicine, including as platforms for processing micro-biomaterials.[18] Thus, using a platform with superhydrophobic surfaces (SH) patterned with wettable superhydrophilic (SL) spots, large amounts of geometrically shaped microgels can be formed through the effect of discontinuous dewetting.[19,20] The high differences in wettability between the SL spots and SH borders lead

to the formation of completely separated water microdroplets (Figure S1A, Supporting Information). The obtained SH-SL polymer layer presents a thickness of 12 μm, and a nanoporous surface (Figure S1B, Supporting Information). Additionally, the Energy Dispersive X-ray Spectroscopy (EDS) mapping of SH-SL microarray shows that SH barriers have enriched Fluor borders, while Sulphur is mainly located on the SL spots (Figure S1C, Supporting Information).

The high-rate production of microgels is shown in Scheme 1. The sacrificial microgel is generated in the SH-SL microarray through an internal gelation approach. Essentially, the ionic crosslinking of alginate hydrogel is mediated by a pH lowering through the hydrolysis of D-glucono-δ-lactone (GDL) into gluconic acid. Under acidic conditions, the insoluble calcium carbonate ($CaCO_3$) salt dispersed in alginate solution starts to release free calcium ions, which enables the gradual gelation. It is noteworthy that cell viability is not affected by the slight decrease in pH.[21,22] This methodology allows the *in situ* crosslinking of alginate in a single SH-SL microarray without using the sandwich method, which requires a precise alignment between microarray containing the $CaCl_2$ solution with the opposite microarray containing the alginate micro-droplets, for the external crosslinking.[23] Additionally, it avoids the use of potentially toxic or denaturizing agents widely used to crosslink hydrogels, such as UV light irradiation or high temperatures. Such strategies can create an unfavorable and chemically reactive environment, which reduces cell viability and may even cause DNA damage.[24,25]

The extreme wettability contrast of SH-SL microarrays allows the breakage of the precursor alginate solution, containing GDL/$CaCO_3$, cells, and μPCL, into thousands of microgels, without requiring manual pipetting or robotic devices. Such platforms are promising for the scalable manufacturing of modular liquefied microcapsule units since they present facile fabrication, compared to other strategies, including those requiring crosslinking baths and/or microfluidics apparatus. Additionally, the post-processing steps applied to form free-standing

liquefied microcapsules, namely the layer-by-layer procedure and the core liquefication with EDTA, are rapid and cost-effective processes. Importantly, each processing step is performed for all microgels at the same time, decreasing time consuming procedures that leverage the scale-up of the developed methodology.

To create microgels, a large droplet of alginate containing cells and μPCL was applied onto the SH-SL patterned surface, and spread by discontinuous dewetting. For the first time, the internal gelation approach was conceived to produce microgels incorporating cells and microparticles to be used as templates for the liquefied capsules assembly.[22] After *in situ* crosslinking of alginate (5 min at 37 ºC), freestanding microgels were slowly detached when immersed in a PBS solution. Subsequently, a multilayered membrane was built through the Layer-by-Layer (LbL) technique. This technique has been widely used to coat the surface of 3D structures for TE applications.[26] The fabrication of the multilayered membrane is based on electrostatic interactions of oppositely charged polyelectrolytes, being "permselective" to relevant bioproducts (e.g. nutrients, oxygen, metabolites, and waste products), and avoiding the entrance of larger components (e.g. immunoglobulins, and immune cells). Through the LbL technique it is possible to generate drug-releasing membranes able to deliver in a timely and controlled manner small molecules, as therapeutic drugs or nucleic acids, for biomedical applications.[27] In this particular case, LbL was applied to produce polymeric multilayered capsules, using three different polyelectrolytes, namely poly-L-lysine, alginate, and chitosan. We already validated the permeability of the LbL membrane. Previous work demonstrated that the multilayered membrane allowed the diffusion of osteogenic differentiation factors added to the culture medium, directing the *in vitro* pre-osteogenic stimulation of encapsulated stem cells.[15] Furthermore, molecular factors such as vascular endothelial growth factor and osteopontin released by encapsulated cells were measured and detected in the culture medium, and thus indicating that cytokines released by the encapsulated cells were able to cross the multilayered membrane of capsules to the outside.[17] After polymeric sequential deposition

on the surface of a sacrificial template, the core was eliminated.[28,29] Therefore, to obtain a liquefied core where cells can co-assemble and build their own tissue-like 3D microenvironment, microgels surrounded by the multilayered membrane were immersed in ethylenediaminetetraacetic acid solution (EDTA). EDTA is a divalent ion chelator, which sequesters the calcium ions acting as crosslinkers of the sacrificial alginate microgel, thus liquefying the inner part of the alginate microgels.

Figure 1A shows the broad ability to develop several microgels with geometrically-controlled shape using the SH-SL microarray. The novelty relies on the fact that it is possible to control the template geometry while they are produced on a large number and on a micro scale. Depending on the photomask design, diverse geometries and different sizes of microgels can be produced. After the production of microgels, it is easy to manipulate and transfer them by pipetting. Here, we demonstrate that besides the classical spherical cell encapsulation systems, it is possible to produce objects with a squared and circular cross-section (**Figure 1B**). To produce circles and squares, the diameter's size of the used photomask was 2520 and 2460 µm, respectively (Figure S2, Supporting Information). Once measured the diameters of circles and squares before and after liquefaction, it is possible to state that there are not statistical differences between them. As expected, there is a slight decrease of the diameter's average of microgels after liquefaction, in both circle and square geometries (**Figure 1C**). Simply by changing the shape's diameter in the photomask, it is possible to create microgels with various sizes. Regarding the analysis in the z-direction, microgels have a convex shape presenting a thickness around 300 µm (Figure S3, Supporting Information). Adipose-derived stromal cells (ASCs) and µPCL were co-encapsulated within multi-shaped microgels. The parameters were set-up to $3x10^6$ of ASCs and 30 mg of µPCL per mL of alginate solution. The surface of µPCL was previously functionalized by combining air-plasma treatment and coating with collagen I, to enhance cell adhesion. ASCs are widely used for TE strategies due to their multilineage differentiation potential, and have a relatively simple process of

accessing and isolating, being available in large quantities with minimal donor site morbidity.[30] Driven by the fact that living tissues are characterized by an appropriate architectural organization of repetitive functional units, the proposed liquefied capsules with different geometries could be valuable for the development of artificial tissues *in vitro*. Such technology could allow the design of muscle fibers or blood vessels *in vitro*, simply by fabricating cylinder-shaped liquefied hydrogels, or could even propose a 3D multilayer hepatic lobule-like tissue, by developing hepatocyte plate's shaped liquefied capsules. Without compromising the advantages of the proposed cell encapsulation system, other type of cells and microparticles can be encapsulated in accordance with the desire tissue to repair, which broads the applicability of this system for multiple TE applications.

After production of capsules, the liquefying process was evaluated. Firstly, we produced microgels encapsulating µPCL stained with nile red. Then, the core was liquefied in a mild process using EDTA. **Figure 2A** shows that the nile red-µPCL were well distributed in the microgels before liquefaction. After liquefaction, regions with higher concentration of the microparticles could be noticed due to the immersion of microparticles in the liquid environment. Additionally, to evidence the successful core liquefaction, liquefied microgels encapsulating only µPCL were placed on top of a 2D culture of ASCs. The nuclei of cells were stained with DAPI (blue). Results showed that liquefied microgels presented a transparent core, and thus it was possible to observe blue spots through the square-shaped microgels, corresponding to the nuclei of externally 2D cultured ASCs. On the other hand, non-liquefied microgels presented an opaque core with autofluorescence, disallowing the observation of the ASCs 2D culture through its polymeric matrix. Liquefied microgels encapsulating nile red-µPCL were also fixed in a gelatin-methacryloyl (GelMA) hydrogel. Following the hydrogel tilt towards a vertical direction (**Figure 2B**), µPCL slowly sinked and agglomerated at the bottom of the liquefied microgels by the effect of gravity (Movie S1, Supporting Information). The ability of the encapsulated microparticles to freely move inside

the liquefied microgel occurs without compromising the mechanical integrity of the system, which is maintained by the presence of a permselective membrane. The liquefied core also allows dynamic stimuli by simply using stirring flaks, as we recently demonstrated.[17] Moreover, the liquefied core confers the ability to adapt to structures with irregular shapes, such as tissue defects, while also allowing minimally implantation procedures by injection. After implantation, the presence of the multilayered membrane avoids the dispersion of the core contents to peripheral regions of the body.

Microgels encapsulating living cells were also produced, to assess cell viability, proliferation, and structural organization. Live-dead assay shows that after 21 days of culture the majority of encapsulated cells remained viable (**Figure 3A**). The metabolic activity of encapsulated cells was evaluated by MTS colorimetric assay at 1, 4, 7, 14, and 21 days of culture. Results indicate that formazan absorbance was significantly higher after 7 days post-encapsulation, with a slight decrease over time (**Figure 3B**). The DNA content significantly increased during the 21 days of culture, indicating the ability of liquefied microgels to support cell proliferation (**Figure 3B**). Importantly, these results also highlight the mild conditions of the proposed cell encapsulation technique. In fact, we already had verified the superior bioperformance of such cell encapsulation systems compared to classical hydrogels.[12,15–17] These reports evidence the ability of liquefied capsules for long-term cell survival, a major challenge for TE strategies aiming cell encapsulation. Such results were confirmed for the encapsulation of different phenotypes of cells, such as L929, human mesenchymal-derived stromal cells, human endothelial cells, human osteoblasts, among others. The fluorescence staining of F-actin filaments (**Figure 3C**) evidenced the interaction and structural organization of the encapsulated cells with the μPCL after 7 days of culture. In the three different geometries, it was possible to observe microaggregates of cells and μPCL.

Overall, the present study proposes the high-throughput fabrication of cell encapsulation microsystems with geometrically-controlled shapes using superhydrophobic-superhydrophilic

microarrays, as processing platform where microgels are crosslinked *in situ*. Such liquefied microgels can potentially be explored as building blocks for bottom-up strategies using the concept of modular TE. This system has a strong modular character, and thus each component can be easily adapted to fulfil the requirements for the bioengineering of multiple tissues or be applied as bioengineered cell-containing constructs for basic biological research and *in vitro* platforms for disease modelling and drug screening. The idea is to use the well-established cell friendly environment provided by such microgels to create more close-to-native systems owning high heterogeneity, while providing multifunctional and adaptive inputs.

Experimental Section

Detailed information is provided in the Supporting Information.

SH-SL micro-arrays: The methodology followed to produce SH-SL micro-arrays has already been reported in literature.[19,23,31] The reader is referred to the Supporting Information.

Production of the loaded microgels: To prepare microgels containing cells and µPCL, 1.5 % w/v of low viscosity sodium alginate from brown algae (9.5 cP, ALG, Merck) was prepared in sodium chloride solution (0.15 M, NaCl, LabChem) containing 2-(N-morpholino)ethanesulfonic acid hydrate (0.025 M, MES, Merck). Afterwards, 30 mg of µPCL and a suspension of $CaCO_3$ (3.65 mg, Fluka) were added per mL of alginate solution. For hydrogel crosslinking, D-glucono-δ-lactone (21.78 mg, GDL, Merck) was added and the mixture was vortexed for 5 min. ASCs were resuspended ($3x10^6$ cells mL^{-1}) in the alginate solution and the mixture was dispersed over the SH-SL slide using the effect of discontinuous dewetting. Then, each slide with different geometries was incubated for 5 min at 37 ºC for a faster gelation. Following crosslinking, the slide was immersed in a NaCl/MES solution for

10 min at room temperature (RT). Here, microgels with different geometries were easily detached from the slide, forming freestanding microgels encapsulating cells and μPCL. Afterwards, a multilayered membrane was formed around the microgel, through the layer-by-layer technique. Poly-L-lysine, alginate, and chitosan were used as polyelectrolytes (0.5 mg mL^{-1}), creating a 12-layered membrane. Ultimately, the liquefied core was obtained by chelation with ethylenediaminetetraacetic acid (5 mM, EDTA, Merck) for 5 min at RT. The pH of all solutions was set to 6.7, excepting for chitosan (pH 6.3). All polyelectrolytes were sterilized by filtration using a 0.22 μm filter. $CaCO_3$ suspension was autoclaved previously.

Supporting Information
Supporting Information is available from the Wiley Online Library or from the author.

Acknowledgements
The authors acknowledge the financial support given by the Portuguese Foundation for Science and Technology (FCT) with the doctoral grant of Sara Nadine (SFRH/BD/130194/2017), the projects "CIRCUS" (PTDC/BTM-MAT/31064/2017) and "MIMETIc" (PTDC/BTM-MAT/31210/2017), and the European Research Council for project "ATLAS" (ERC-2014-AdG-669858). The authors also acknowledge funding from national funds (OE), through FCT, in the scope of the framework contract foreseen in the numbers 4, 5 and 6 of the article 23, of the Decree-Law 57/2016, of August 29, changed by Law 57/2017, of July 19. This work was also partly supported by Japan Society for the Promotion of Science (JSPS) Bilateral Open Partnership Joint Research Projects. This work was developed within the scope of the project CICECO-Aveiro Institute of Materials, UIDB/50011/2020 & UIDP/50011/2020, financed by national funds through the FCT/MEC and when appropriate co-financed by FEDER under the PT2020 Partnership Agreement.

Received: ((will be filled in by the editorial staff))
Revised: ((will be filled in by the editorial staff))
Published online: ((will be filled in by the editorial staff))

References

1. Causa, F., Netti, P.A., and Ambrosio, L. (2007) A multi-functional scaffold for tissue regeneration: The need to engineer a tissue analogue. *Biomaterials*, **28** (34), 5093–5099.
2. Gaspar, V.M., Lavrador, P., Borges, J., Oliveira, M.B., and Mano, J.F. (2020) Advanced Bottom-Up Engineering of Living Architectures. *Adv. Mater.*, **32** (6),

1903975.

3. Correia, C.R., Reis, R.L., and Mano, J.F. (2018) Design Principles and Multifunctionality in Cell Encapsulation Systems for Tissue Regeneration. *Adv. Healthc. Mater.*, **7** (19), e1701444.
4. Zhang, S. (2003) Fabrication of novel biomaterials through molecular self-assembly. *Nat. Biotechnol.*, **21** (10), 1171–1178.
5. Annabi, N., Tamayol, A., Uquillas, J.A., Akbari, M., Bertassoni, L.E., Cha, C., Camci-Unal, G., Dokmeci, M.R., Peppas, N.A., and Khademhosseini, A. (2014) 25th Anniversary Article: Rational Design and Applications of Hydrogels in Regenerative Medicine. *Adv. Mater.*, **26** (1), 85–124.
6. Li, F., Truong, V.X., Fisch, P., Levinson, C., Glattauer, V., Zenobi-Wong, M., Thissen, H., Forsythe, J.S., and Frith, J.E. (2018) Cartilage tissue formation through assembly of microgels containing mesenchymal stem cells. *Acta Biomater.*, **77**, 48–62.
7. Liu, Z., Takeuchi, M., Nakajima, M., Hu, C., Hasegawa, Y., Huang, Q., and Fukuda, T. (2017) Three-dimensional hepatic lobule-like tissue constructs using cell-microcapsule technology. *Acta Biomater.*, **50**, 178–187.
8. Naito, H., Melnychenko, I., Didie, M., Schneiderbanger, K., Schubert, P., Rosenkranz, S., Eschenhagen, T., and Zimmermann, W.-H. (2006) Optimizing engineered heart tissue for therapeutic applications as surrogate heart muscle. *Circulation*, **114** (1 Suppl), I72-8.
9. Correia, C.R., Nadine, S., and Mano, J.F. (2020) Cell Encapsulation Systems Toward Modular Tissue Regeneration: From Immunoisolation to Multifunctional Devices. *Adv. Funct. Mater.*, **n/a** (n/a), 1908061.
10. Li, Y., Poon, C.T., Li, M., Lu, T.J., Pingguan-Murphy, B., and Xu, F. (2015) Hydrogel Fibers: Chinese-Noodle-Inspired Muscle Myofiber Fabrication (Adv. Funct. Mater. 37/2015). *Adv. Funct. Mater.*, **25** (37), 6020.

11. Lee, K.H., Shin, S.J., Park, Y., and Lee, S.-H. (2009) Synthesis of cell-laden alginate hollow fibers using microfluidic chips and microvascularized tissue-engineering applications. *Small*, **5** (11), 1264–1268.

12. Correia, C.R., Reis, R.L., and Mano, J.F. (2013) Multilayered Hierarchical Capsules Providing Cell Adhesion Sites. *Biomacromolecules*, **14** (3), 743–751.

13. Sheehy, E.J., Kelly, D.J., and O'Brien, F.J. (2019) Biomaterial-based endochondral bone regeneration: a shift from traditional tissue engineering paradigms to developmentally inspired strategies. *Mater. Today Bio*, **3**, 100009.

14. Jeon, O., Powell, C., Ahmed, S.M., and Alsberg, E. (2010) Biodegradable, photocrosslinked alginate hydrogels with independently tailorable physical properties and cell adhesivity. *Tissue Eng. Part A*, **16** (9), 2915–2925.

15. Correia, C.R., Pirraco, R.P., Cerqueira, M.T., Marques, A.P., Reis, R.L., and Mano, J.F. (2016) Semipermeable Capsules Wrapping a Multifunctional and Self-regulated Co-culture Microenvironment for Osteogenic Differentiation. *Sci. Rep.*, **6** (1), 21883.

16. Correia, C.R., Gil, S., Reis, R.L., and Mano, J.F. (2016) A Closed Chondromimetic Environment within Magnetic-Responsive Liquified Capsules Encapsulating Stem Cells and Collagen II/TGF-β3 Microparticles. *Adv. Healthc. Mater.*, **5** (11), 1346–1355.

17. Nadine, S., Patrício, S.G., Correia, C.R., and Mano, J.F. (2019) Dynamic microfactories co-encapsulating osteoblastic and adipose-derived stromal cells for the biofabrication of bone units. *Biofabrication*, **12** (1), 15005.

18. Lima, A.C., and Mano, J.F. (2015) Micro/nano-structured superhydrophobic surfaces in the biomedical field: part II: applications overview. *Nanomedicine (Lond).*, **10** (2), 271–297.

19. Feng, W., Li, L., Ueda, E., Li, J., Heißler, S., Welle, A., Trapp, O., and Levkin, P.A. (2014) Surface Patterning via Thiol-Yne Click Chemistry: An Extremely Fast and Versatile Approach to Superhydrophilic-Superhydrophobic Micropatterns. *Adv. Mater.*

Interfaces, **1** (7), 1400269.

20. Ueda, E., Geyer, F.L., Nedashkivska, V., and Levkin, P.A. (2012) DropletMicroarray: facile formation of arrays of microdroplets and hydrogel micropads for cell screening applications. *Lab Chip*, **12** (24), 5218–5224.
21. Fonseca, K.B., Bidarra, S.J., Oliveira, M.J., Granja, P.L., and Barrias, C.C. (2011) Molecularly designed alginate hydrogels susceptible to local proteolysis as three-dimensional cellular microenvironments. *Acta Biomater.*, **7** (4), 1674–1682.
22. Bidarra, S.J., Barrias, C.C., Fonseca, K.B., Barbosa, M.A., Soares, R.A., and Granja, P.L. (2011) Injectable in situ crosslinkable RGD-modified alginate matrix for endothelial cells delivery. *Biomaterials*, **32** (31), 7897–7904.
23. Neto, A.I., Demir, K., Popova, A.A., Oliveira, M.B., Mano, J.F., and Levkin, P.A. (2016) Fabrication of Hydrogel Particles of Defined Shapes Using Superhydrophobic-Hydrophilic Micropatterns. *Adv. Mater.*, **28** (35), 7613–7619.
24. Mironi-Harpaz, I., Wang, D.Y., Venkatraman, S., and Seliktar, D. (2012) Photopolymerization of cell-encapsulating hydrogels: Crosslinking efficiency versus cytotoxicity. *Acta Biomater.*, **8** (5), 1838–1848.
25. Nguyen, K.T., and West, J.L. (2002) Photopolymerizable hydrogels for tissue engineering applications. *Biomaterials*, **23** (22), 4307–4314.
26. Borges, J., and Mano, J.F. (2014) Molecular Interactions Driving the Layer-by-Layer Assembly of Multilayers. *Chem. Rev.*, **114** (18), 8883–8942.
27. Costa, R.R., Alatorre-Meda, M., and Mano, J.F. (2015) Drug nano-reservoirs synthesized using layer-by-layer technologies. *Biotechnol. Adv.*, **33** (6 Pt 3), 1310–1326.
28. Ariga, K., Lvov, Y.M., Kawakami, K., Ji, Q., and Hill, J.P. (2011) Layer-by-layer self-assembled shells for drug delivery. *Adv. Drug Deliv. Rev.*, **63** (9), 762–771.
29. De Koker, S., De Cock, L.J., Rivera-Gil, P., Parak, W.J., Auzely Velty, R., Vervaet, C.,

Remon, J.P., Grooten, J., and De Geest, B.G. (2011) Polymeric multilayer capsules delivering biotherapeutics. *Adv. Drug Deliv. Rev.*, **63** (9), 748–761.

30. Dai, R., Wang, Z., Samanipour, R., Koo, K., and Kim, K. (2016) Adipose-Derived Stem Cells for Tissue Engineering and Regenerative Medicine Applications. *Stem Cells Int.*, **2016**, 6737345.

31. Geyer, F.L., Ueda, E., Liebel, U., Grau, N., and Levkin, P.A. (2011) Superhydrophobic–Superhydrophilic Micropatterning: Towards Genome-on-a-Chip Cell Microarrays. *Angew. Chemie Int. Ed.*, **50** (36), 8424–8427.

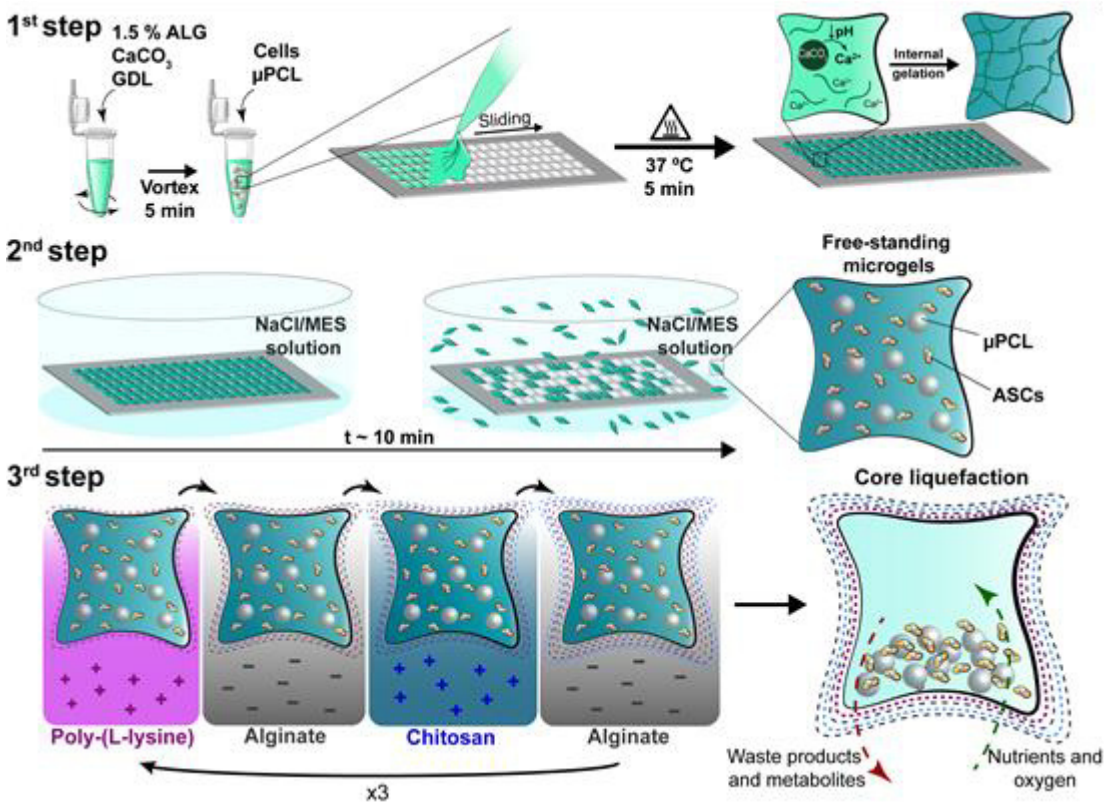

Scheme 1. Schematic representation of the high-throughput fabrication of liquefied and multilayered capsules with defined sizes and shapes, and encapsulating cells and surface-modified polycaprolactone microparticles (µPCL). 1st step: Microgel formation by internal and controlled crosslinking of alginate, upon deposition of the liquid precursor onto a superhydrophobic-superhydrophilic microarray. 2nd step: After complete gelation, freestanding microgels encapsulating cells and µPCL are obtained by detachment in a sodium chloride solution containing 2-(N-morpholino)ethanesulfonic acid hydrate (NaCl/MES). 3rd step: Layer-by-layer is subsequently performed using poly(L-lysine), alginate, and chitosan as polyelectrolytes in order to obtain a 12-layered membrane. Ultimately, the core is liquefied after immersion in ethylenediaminetetraacetic acid solution (EDTA).

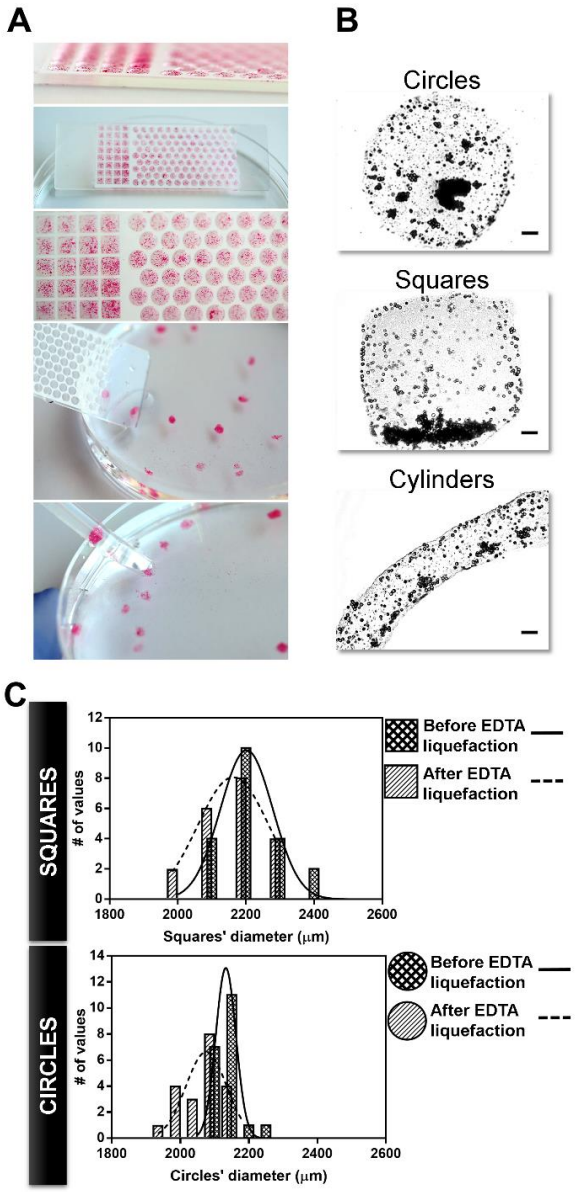

Figure 1. A. Array of circle- and square-shaped microgels production encapsulating nile red stained polycaprolactone microparticles (µPCL). Microgels are obtained by the effect of discontinuous dewetting on the superhydrophobic-superhydrophilic (SH-SL) microarray. The freestanding microgels are acquired after immersion of SH-SL microarray in a buffer, and can be easily manipulated by pipetting. B. Representative brightfield images of high-shaped microgels encapsulating cells and µPCL. Scale bar: 200 µm. C. Size distribution histogram of square- and circle- shaped microgels, before and after liquefaction with ethylenediaminetetraacetic acid (EDTA).

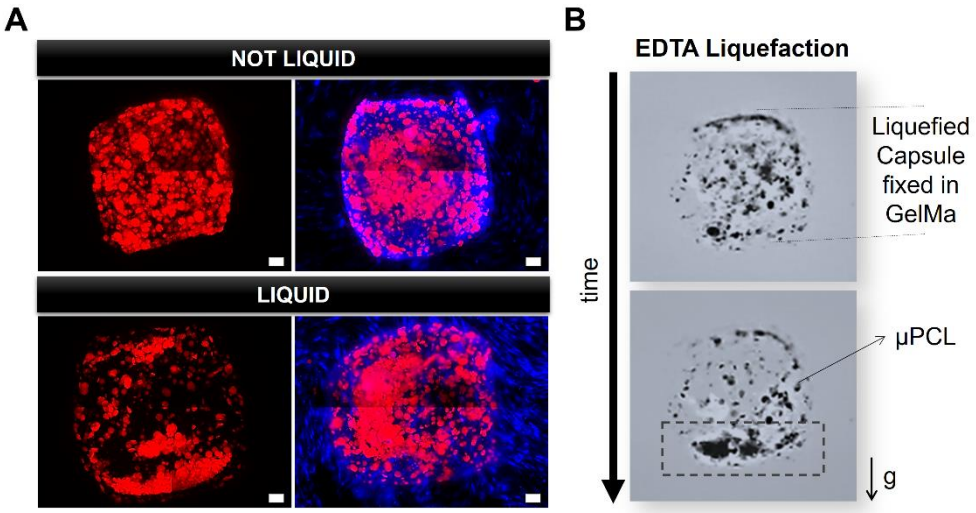

Figure 2. Evaluation of the ethylenediaminetetraacetic acid (EDTA) liquefying process A. Fluorescence images of square-shaped microgels encapsulating nile red polycaprolactone microparticles (µPCL) before and after liquefaction, on left side. On right side, fluorescence images of microgels encapsulating nile red-µPCL placed on the top of a 2D culture of ASCs before and after liquefaction. Nuclei of cells were stained with DAPI (blue). Scale bar: 200 µm. B. Screenshots of the movie (Movie S1, Supporting Information) of microgels entrapped in GelMA. Through the gravity action, µPCL are falling to the bottom of the microgels. The dotted lines represent the accumulation of µPCL.

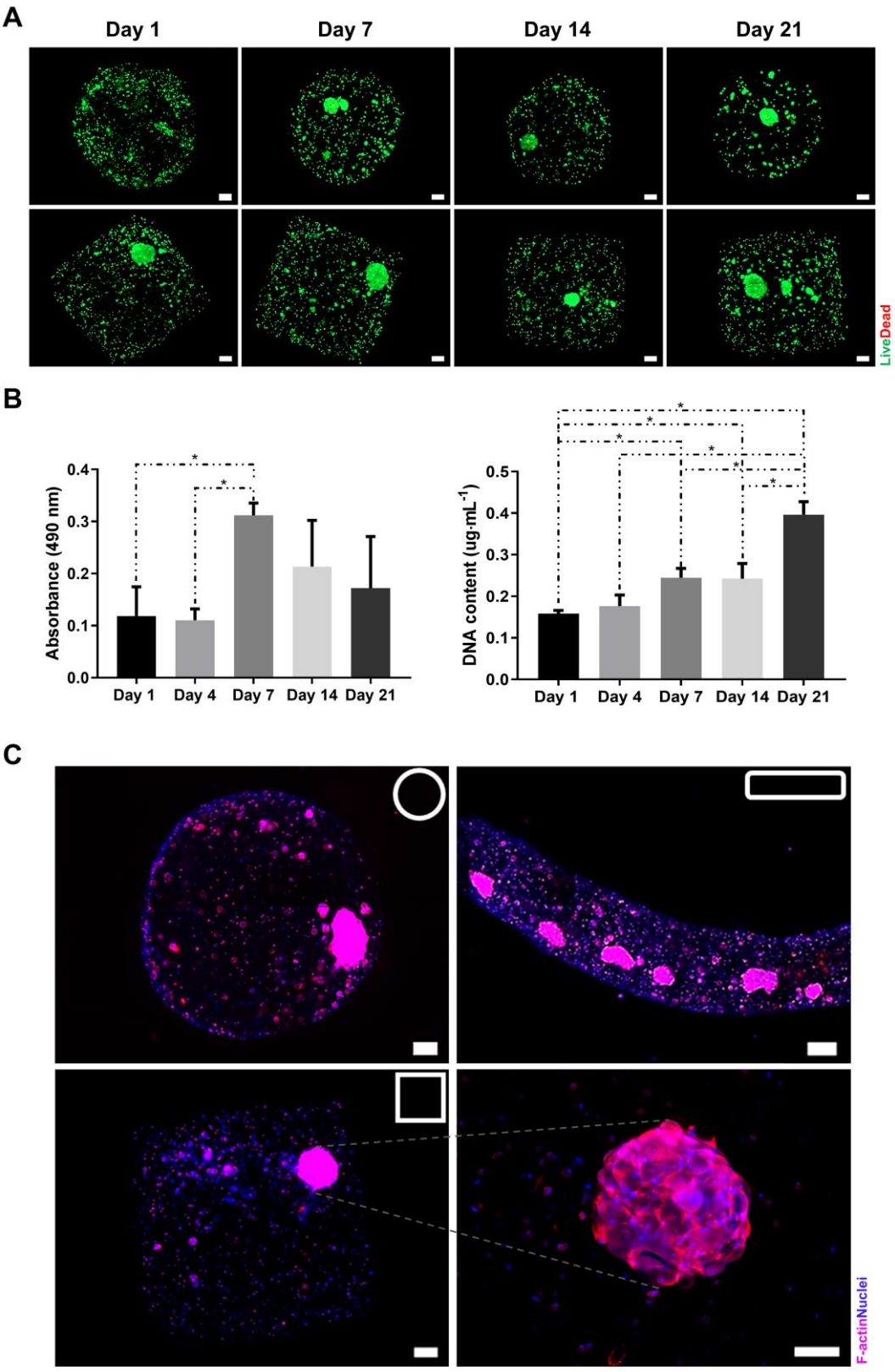

Figure 3. A. Live-dead fluorescence assay of microgels encapsulating adipose-derived stromal cells (ASCs) and polycaprolactone microparticles (µPCL) after 1, 7, 14, and 21 days of culture. Living cells are stained by calcein (green) and dead cells by propidium iodide (red). Scale bars: 200 µm. B. Cell metabolic activity determined by MTS colorimetric assay and cell proliferation by DNA quantification. *p*-values <0.05 are considered statistically

significant. C. DAPI-phalloidin fluorescence assay of circle, square and cylindrical capsules after 7 days of culture. Cells nuclei are stained by DAPI (blue) and F-actin filaments by phalloidin (pink). Scale bars: 200 μm, excepting bottom-right image: 100 μm.

Table of Contents

Liquefied Capsules

S. Nadine, S. G. Patrício, C. C. Barrias, I. S. Choi, M. Matsusaki, C. R. Correia*, J. F. Mano*

Geometrically controlled liquefied capsules for modular tissue engineering strategies

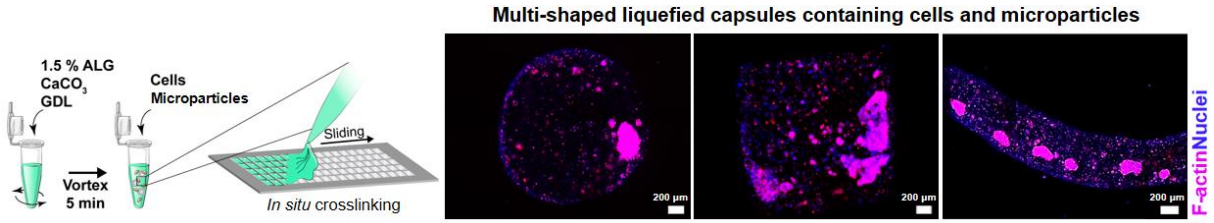

The concept relies on the high-throughput production of alginate-based microgels with defined geometries, using an *in situ* crosslinking procedure. Such encapsulation system is surrounded by a permselective polymeric membrane which wraps cells and microparticles in a liquefied environment. The proposed system can potentially be explored as building blocks for bottom-up strategies within the concept of modular tissue engineering.

Supporting Information

Geometrically controlled liquefied capsules for modular tissue engineering strategies

Sara Nadine, Sónia G. Patrício, Cristina C. Barrias, Insung S. Choi, Michiya Matsusaki, Clara R. Correia, João F. Mano**

E-mail: claracorreia@ua.pt and jmano@ua.pt

Experimental Section S1.

Processing and characterization of SH-SL micro-arrays: The methodology followed to produce SH-SL micro-arrays has already been reported in literature.[19,23,31] Briefly, glass microscope slides were activated by immersion in 1 M sodium hydroxide (NaOH, Eka) for 1 h, followed by neutralization in 1 M hydrochloric acid (HCl, Sigma-Aldrich) for 30 min. After activation, the glass slides were modified with 20% v/v solution of 3-(trimethoxysilyl)propyl methacrylate (Sigma-Aldrich) in ethanol for 30 min at room temperature (RT). Afterwards, activated glass slides were placed in a vacuumed desiccator (50 mbar, 3-5 h) under trichloro(1H,1H,2H,2H-perfluorooctyl)silane (Sigma-Aldrich) atmosphere. Then, to create a thin polymer layer over the fluorinated glass slide, a polymerization mixture solution was prepared with 2- hydroxyethyl methacrylate (24 wt%, HEMA, Sigma-Aldrich), ethylene dimethacrylate (16 wt%, EDMA, Sigma-Aldrich), 1-decanol (12 wt%, Sigma-Aldrich), cyclohexanol (48 wt%, Sigma-Aldrich), and 2,2-dimethoxy-2-phenylacetophenone (0.4 wt%, DMPA, Sigma-Aldrich). To define the thickness of the polymer layer, two 12.5 μm thin strips of aluminium foil were applied on the corners of a fluorinated glass slide. Subsequently, the polymerization solution was applied over the fluorinated glass slide, and a methacrylated glass slide was clamped on top of it. The polymerization was performed under 264 nm of UV radiation for 15 min and with 12 mW cm^{-}

^{2} of intensity. After ethanol washing and nitrogen stream drying, the polymer layer was modified with 4-pentynoic acid via standard esterification. The esterification solution was prepared using dichloromethane (45 mL, Sigma-Aldrich), 4-(dimethylamino)pyridine (56 mg, Acros Organics), pentynoic acid (111.6 mg, Acros Organics), and of N,N'-diisopropylcarbodiimine (180 µL, Acros Organics), in continuous stirring for 4 h at RT. Ultimately, SH patterns with specific geometries were obtained by applying 5% v/v solution of 1H,1H,2H,2H-perfluorodecanethiol (PFDT, Sigma-Aldrich) in acetone onto the polymer surface, followed by UV irradiation (264 nm) through a quartz photomask at 12 mW cm^{-2} for 1 min. The remaining alkyne groups were subjected to a thiol-yne reaction with 2-mercaptoethanol (10 % v/v, Alfa Aesar) under 264 nm of UV radiation for 15 min and with 12 mW cm^{-2} of intensity, originating the formation of SL areas.

Functionalized PCL microparticles: Poly(ε-caprolactone) microparticles (µPCL) were produced by emulsion solvent evaporation technique. Briefly, PCL (5 % w/v PCL, Mw ~ 80000, Merck) was dissolved in methylene chloride (Honeywell). To obtain stained µPCL, nile-red (0.02% w/v, Sigma-Aldrich) was added to this solution. The PCL solution was slowly added to a stirring 0.5 % w/v polyvinyl alcohol (PVA, Merck) solution. Under agitation during 2 days at RT, the produced µPCL were subsequently sieved to obtain a diameter range between 40-50 µm. The obtained µPCL presented a diameter of 45.7 ± 7.3 µm. Afterwards, surface modification was performed by placing µPCL into a low pressure plasma reactor chamber (ATTO, Diener Electronic) fitted with a radio frequency generator. Air was used as gas atmosphere. A low-pressure glow discharge was generated at 30 V and 0.2-0.4 mbar for 15 min. Then, µPCL were immediately sterilized by UV-radiation for 30 min, and then immersed in an acetic acid solution (20 mM, Chem-Lab NV) containing collagen I (10 µg cm^{-2}, rat protein tail, ThermoFisher Scientific) for 4 hours at RT.

Adipose stem cells culture: Adipose-derived stromal cells (ASCs, passage 6, ATCC® PCS-500-011™) were cultured in α-MEM (minimum essential medium, ThermoFisher Scientific), supplemented with 10 % of heat-inactivated fetal bovine serum (FBS, ThermoFisher Scientific), 100 U mL^{-1} of penicillin and 0.1 mg mL^{-1} of streptomycin (ThermoFisher Scientific). For cell encapsulation purposes, ASCs were washed with PBS solution and detached using Tripsin-EDTA (Merck) for 5 min at 37ºC. Cells were counted and added to the alginate solution.

Cellular viability: To assess the viability of encapsulated ASCs, LiveDead fluorescence assay and mitochondrial metabolic activity quantification were performed according to the manufacturer's recommendation (ThermoFisher Scientific). Briefly, for LiveDead dead assay, each sample was stained with calcein-AM (1:500 in PBS) and propidium iodide (1:1000 in PBS), for 15 min at 37 ºC, and protected from light. Afterwards, samples were immediately visualized by fluorescence microscopy (Axio Imager 2, Zeiss). The mitochondrial metabolic activity quantification was performed using an MTS colorimetric assay (CellTiter96®, AQueous One Solution Cell, Promega) according to the manufacturer's recommendation. Briefly, samples were incubated protected from light with the reagent kit (1:6 in PBS) for 4 h at 37 ºC in a humidified 5 % CO2 air atmosphere. Then, absorbance was read at a wavelength of 490 nm using a microplate reader (Gen 5, Synergy HT, Biotek).

Cell Proliferation Quantification: Total DNA quantification was performed using the Quant-iTTM PicoGreen® dsDNA assay kit (Life Technologies). Briefly, samples (n = 3 per well in triplicate) were suspended in ultra-pure sterile water (500 µL per well) for cell lysis. After 1 h in a 37 °C shaking water bath, samples were frozen at − 80 °C overnight. Then, samples were defrosted and used according to the manufactures' specifications. A standard curve for DNA analysis was obtained with the provided dsDNA solution. After 10 min of incubation at RT,

fluorescence was read at an excitation wavelength of 485/20 nm and 528/20 nm of emission using a microplate reader (Gen 5 2.01, Synergy HT, Biotek).

Fluorescence staining: In order to evaluate cellular morphology, ASCs were stained for F-actin and nuclei visualization. Samples were washed with PBS and fixed in formaldehyde (4% v/v) for 1 hour at RT. Then, samples were permeabilized with Triton-X (0.1% v/v, Merck) for 5 min, followed by incubation in Flash Phalloidin Red 594 (300 U, 1:40 in PBS, Biolegend) for 45 min at RT. Cells nuclei were counterstained with DAPI (1mg.mL-1, 1:1000 in PBS, ThermoFisher Scientific) for 5 min. Following PBS washing, samples were visualized by fluorescence microscopy (Axio Imager 2, Zeiss).

Diameter measurements: The diameter of shaped non-liquefied or liquefied microgels was measured by ImageJ image analysis software. Each value presented correspond to the average diameter of a total of 15 samples for each condition.

Z-direction measurements: The side view of shaped non-liquefied or liquefied microgels was obtained using the Contact Angle System OCA (Data Physics, Germany; software SCA 20). The thickness of microgels was measured by ImageJ image analysis software. Each value presented correspond to the average diameter of a total of 5 samples for each condition.

Scanning Electron Microscopy and Energy Dispersive X-ray Spectroscopy (SEM-EDS): Morphological and compositional analysis of SH-SL microarray were carried out by scanning electron microscopy (Hitachi S4100, Tokyo, Japan). Energy dispersive X-ray spectroscopy (EDS, Hitachi, SU-70 instrument) was also used to determine the elemental components of the sample's surface. For that, the SH-SL microarray was sputtered with a thin film of carbon

(K950X Turbo-Pumped Carbon Evaporator) and the analysis was made at an accelerating voltage of 15 kV.

Gelatin Methacryloyol (GelMa) synthesis: For GelMa synthesis, 10% w/v gelatin type A (300 bloom, Sigma-Aldrich) derived from porcine skin tissue was dissolved in carbonate-bicarbonate (CB) buffer for 5 h at 40 ºC and 500 rpm. To prepare the CB buffer, 4 mL of 0.2 M anhydrous sodium carbonate, 46 mL of 0.2 M sodium bicarbonate, and 150 mL of distilled water were mixed (pH 9.2). After complete solubilisation of gelatin, pH was set up to 9. Afterwards, 0.1 mL of methacrylic anhydride (MAA, Sigma-Aldrich) was added per gram of gelatin. The polymeric mixture was stirred vigorously and maintained at 40 °C overnight and protected from light. The polymeric solution was then transferred to dialysis membranes made of regenerated cellulose (14 kDa cutoff, Sigma-Aldrich) and dialyzed for 3 days in deionized water refreshed each 3 h. GelMA solution was then frozen at −80 °C and lyophilized. 5% w/v lyophilized GelMa was dissolved in a solution of 1% w/v lithium phenyl-2,4,6-trimethylbenzoylphosphinate (LAP, Sigma-Aldrich) in NaCl/MES. To entrap liquefied capsules, the polymer solution was laid over microgels in petri dishes, followed by UV irradiation (0.16 W cm^{-2}) for 120 s.

Statistical analysis: Statistical analysis was performed using two-way analysis of variance (ANOVA) with Turkey's post-hoc test (GraphPad Prism 6.0). *p*-values <0.05 were considered statistically significant (*p<0.05). All results are presented as mean ± standard deviation.

Figure S1A shows the high difference in wettability between the SL spots and SH borders, leading to the spontaneous formation of completely separated transparent water microdroplets. These SH-SL patterned microarrays were obtained by synthetizing onto a glass slide a thin nanoporous polymeric film functionalized with the reactive alkyne groups incorporated from a standard sterification (Figure S1B). Applying a photomask with a specific geometry, the unprotected alkyne surface reacts with 1H,1H,2H,2H-perfluorodecanethiol forming a grid-like superhydrophobic pattern with enriched Fluor borders, while the following photoclick reaction of the with 2-mercaptoethanol leads to the formation of Sulphur-enriched SL spots (Figure S1C).

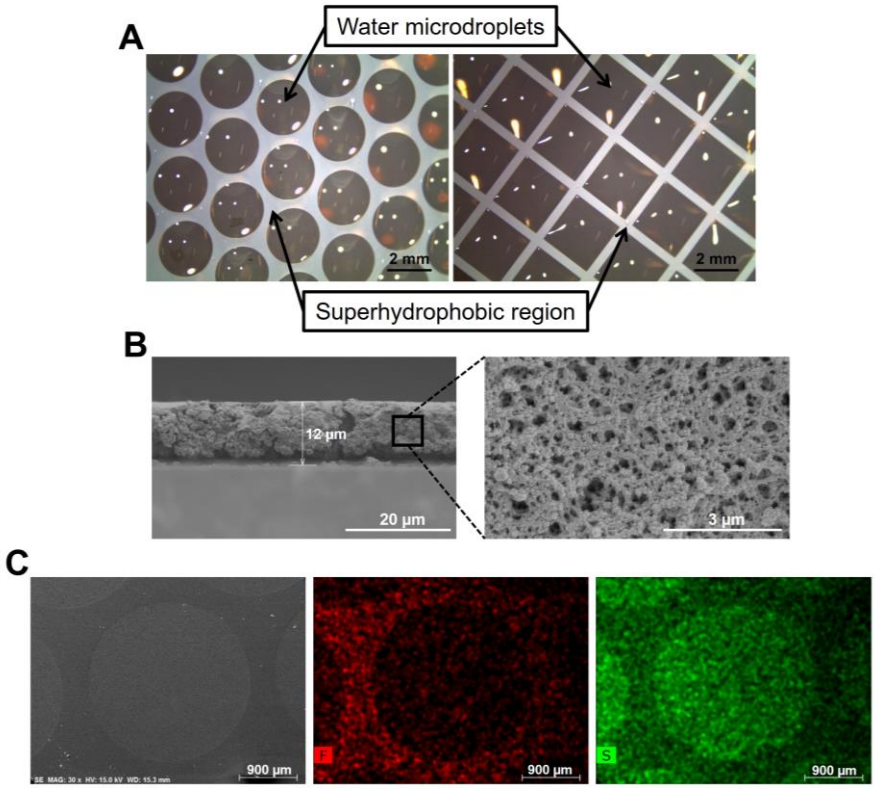

Figure S1. A. Optical images of droplet superhydrophilic microarrays formation with circular- or square-shaped geometries. A large droplet of water was applied onto the superhydrophobic-superhydrophilic (SH-SL) patterned surface, and spread by discontinuous dewetting. **B.** SEM cross-section and surface morphology of the nanoporous polymeric film.

C. SEM image of a circular SH-SL patterned surface, and the correspondent EDS mapping of Fluor (red) and Sulphur (green), key elements of the thiols used for the formation of either superhydrophobic or superhydrophilic surfaces.

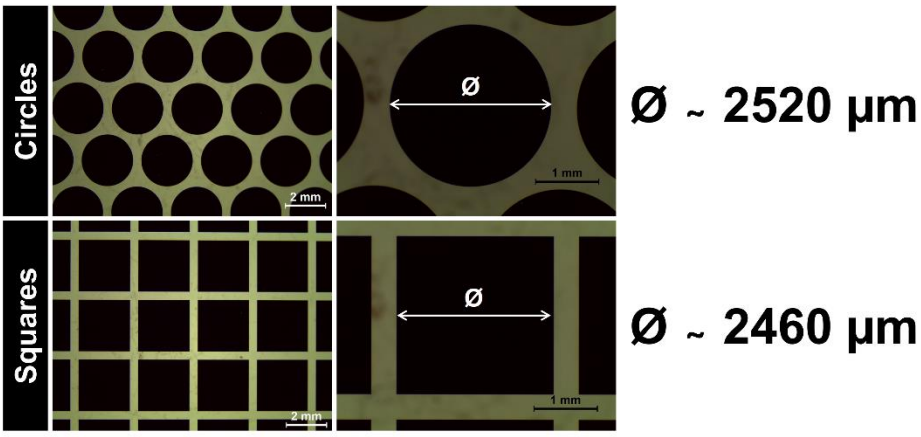

Figure S2. Optical microscope images of circular- and square-shaped superhydrophilic arrays. Measurements were performed using the ImageJ software.

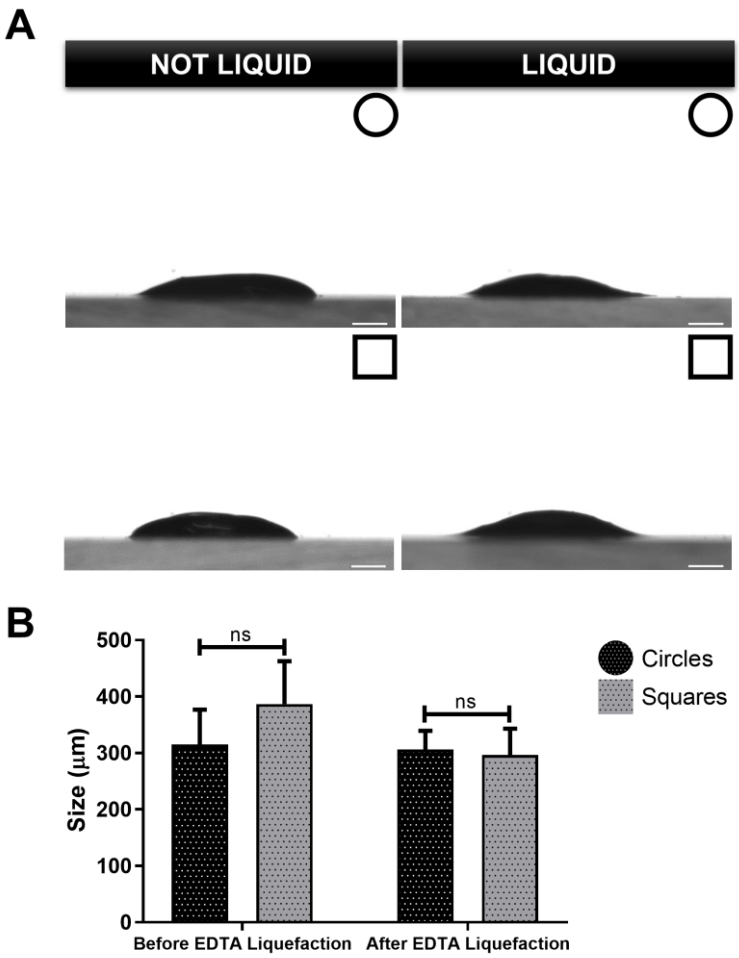

Figure S3. A. Representative side views of the circular- and square-shaped microgels, before and after the liquefaction process with ethylenediaminetetraacetic acid (EDTA). Scale bars: 500 µm. **B.** Thickness of square- and circle- shaped microgels. Measurements were performed before and after EDTA liquefaction. Results were marked as non-significant (ns) for *p-values* > 0.05.